

Electrostatic Polarization Makes a Substantial Contribution to the Free Energy of Avidin–Biotin Binding

Yan Tong,^{†,‡} Ye Mei,^{*,†,¶} Yong L. Li,[§] Chang G. Ji,^{†,¶} and John Z. H. Zhang^{*,†,¶,||}

Institute of Theoretical and Computational Science and State Key Laboratory of Precision Spectroscopy, Department of Physics, East China Normal University, Shanghai 200062, China, School of Pharmacy, Henan University of Traditional Chinese Medicine, Zhengzhou 450008, China, Key Laboratory of Mesoscopic Chemistry of Ministry of Education (MOE), School of Chemistry and Chemical Engineering, Nanjing University, Nanjing 210093, China, and Department of Chemistry, New York University, New York, New York 10003

Received November 11, 2009; E-mail: ymei@phy.ecnu.edu.cn; john.zhang@nyu.edu

Abstract: Avidin–biotin is one of the strongest protein–ligand binding systems, with broad applications in biomedical science. Here we report a quantum-based computational study to help elucidate the mechanism of binding avidin to biotin (BTN1) and its close analogue, 2'-iminobiotin (BTN2). Our study reveals that electronic polarization of protein plays a critical role in stabilizing the β sheet (Thr113-Arg122) at the binding site and makes a substantial contribution to the free energy of avidin–biotin binding. The current finding is in contradiction to the previous notion that electrostatic interaction has no effect on or makes an unfavorable contribution to the free energy of avidin–biotin binding. Our calculations also show that the difference in binding free energy of avidin to BTN1 and BTN2 is almost entirely due to the contribution of electrostatic interaction resulting from polarization-induced stabilization of a hydrogen bond between avidin and BTN1. The current result provides strong evidence that protein polarization accounts for the electrostatic contribution to binding free energy that was missing in previous studies of avidin–biotin binding.

Introduction

Electrostatic interactions play a critical role in determining the structure and function of biomolecules.^{1–4} Thus, the ability to accurately describe the electrostatic interaction is essential for a reliable quantitative description of protein dynamics and for structure–function correlation studies of proteins. Over the past decades, significant progress has been made in the development of molecular mechanics (MM) force fields for biomolecular simulation.^{5–10} However, there is a major deficiency in the standard force fields (nonpolarizable force fields), i.e., the lack of protein polarization. This casts uncertainties on the accuracy and reliability

of computational study of biomolecules, especially in long molecular dynamics (MD) simulation studies. For example, recently Weis et al. noted that a polarizable force field is needed for MM/Poisson–Boltzmann surface area (PBSA) calculation of protein–ligand binding.¹¹ Although progress has been made in the development of polarizable force fields based on classical electrostatic models,^{12,13} their general applications are still lacking due to uncertainty over the accuracy and computational cost.¹⁴

Recent progress in fragment-based quantum mechanical (QM) calculation of protein^{15–26} has opened a new avenue for generating quantum-based electrostatic interactions for biomolecular study. For that purpose, polarized protein-specific charge (PPC) has recently been developed to accurately represent electrostatic interaction in proteins at a given structure (usually at or near the native structure),²⁷ based on a QM fragment method^{28–31} coupled with a continuum solvent model.^{27,31}

[†] Institute of Theoretical and Computational Science, East China Normal University.

[‡] School of Pharmacy, Henan University of Traditional Chinese Medicine.

[¶] State Key Laboratory of Precision Spectroscopy, Department of Physics, East China Normal University.

[§] School of Chemistry and Chemical Engineering, Nanjing University.

^{||} Department of Chemistry, New York University.

- (1) Davis, M. E.; McCammon, J. A. *Chem. Rev.* **1990**, *90*, 509–521.
- (2) Honig, B.; Nicholls, A. *Science* **1995**, *268*, 1144–1149.
- (3) Perutz, M. F. *Science* **1978**, *201*, 1187–1191.
- (4) Matthew, J. B. *Annu. Rev. Biophys. Biophys. Chem.* **1985**, *14*, 387–417.
- (5) Lifson, S.; Warshel, A. *J. Chem. Phys.* **1968**, *49*, 5116–5129.
- (6) Brooks, B. R.; Bruccoleri, R. E.; Olafson, B. D.; States, D. J.; Swaminathan, S.; Karplus, M. *J. Comput. Chem.* **1983**, *4*, 187–217.
- (7) Pearlman, D. A.; Case, D. A.; Caldwell, J. W.; Ross, W. S.; Cheatham, T. E., III; DeBolt, S.; Ferguson, D.; Seibel, G.; Kollman, P. A. *Comput. Phys. Commun.* **1995**, *91*, 1–41.
- (8) Hagler, A. T.; Huler, E.; Lifson, S. *J. Am. Chem. Soc.* **1974**, *96*, 5319–5327.
- (9) Nemethy, G.; Pottle, M. S.; Scheraga, H. A. *J. Phys. Chem.* **1983**, *87*, 1883–1887.
- (10) Berendsen, H. J. C.; Postma, J. P. M.; van Gunsteren, W. F.; DiNola, A.; Haak, J. R. *J. Chem. Phys.* **1984**, *81*, 3684–3690.

- (11) Weis, A.; Katebzadeh, K.; Soderhjelm, P.; Nilsson, I.; Ryde, U. *J. Med. Chem.* **2006**, *49*, 6596–6606.
- (12) Halgren, T. A.; Damm, W. *Curr. Opin. Struct. Biol.* **2001**, *11*, 236–242.
- (13) Kaminski, G. A.; Stern, H. A.; Berne, B. J.; Friesner, R. A.; Cao, Y. X. X.; Murphy, R. B.; Zhou, R. H.; Halgren, T. A. *J. Comput. Chem.* **2002**, *23*, 1515–1531.
- (14) Jorgensen, W. L. *J. Chem. Theory Comput.* **2007**, *12*, 1877–1877.
- (15) Nakano, T.; Kaminuma, T.; Sato, T.; Akiyama, Y.; Uebayasi, M.; Kitaura, K. *Chem. Phys. Lett.* **2000**, *318*, 614–618.
- (16) Gao, J. *J. Phys. Chem. B* **1997**, *101*, 657–663.
- (17) Fedorov, D. G.; Kitaura, K.; Li, H.; Jensen, J. H.; Gordon, M. S. *J. Comput. Chem.* **2006**, *27*, 976–985.
- (18) Zhang, D. W.; Xiang, Y.; Zhang, J. Z. H. *J. Phys. Chem. B* **2003**, *107*, 12039–12041.
- (19) Chen, X. H.; Zhang, Y. K.; Zhang, J. Z. H. *J. Chem. Phys.* **2005**, *122*, 184105.

Previous studies showed that PPC provides a more accurate and reliable description of protein structure and dynamics in pK_a calculation,²⁷ protein–ligand binding,³² stability of hydrogen bonds,^{33,34} and order parameters.³⁵ It has been noted in these studies that the local structure of protein, especially intra-protein hydrogen bonding, is generally more stable under polarized protein-specific force field than standard (nonpolarizable) force fields.^{32,33}

Avidin–biotin is one of the most remarkable protein–ligand binding systems in nature, with a large binding affinity of 20 kcal/mol.³⁶ Thus, elucidating the binding mechanism of this classical system has motivated a variety of biophysical experiments, and this system has been the focus of binding free energy studies.^{11,37,38} In particular, free energy calculation by Kuhn et al. led to the conclusion that association between avidin and biotin is mainly driven by van der Waals interactions, while electrostatic interaction does not contribute to the free energy of binding.^{37,38} This conclusion is somewhat surprising in view of the fact that the ligand biotin is charged and the binding affinity is very large. Since this conclusion is based on MD simulations under standard AMBER force field, it is important to investigate the possible deficiency of the force field and its effect on the calculation of the binding affinity of biotin–avidin. Recently, DeChancie et al. applied a high-level QM calculation to the biotin–avidin system, and they suggested that hydrogen bond cooperativity is essential for this femtomolar binding system.³⁹ However, their QM calculation is based on a static structure; dynamic effects were not taken into account. In the current study, we employ quantum-based PPC to investigate the effect of protein polarization on avidin binding to biotin and its analogue using MD simulations. Two issues will be addressed here: (1) How is the structure of the avidin–biotin complex affected by protein polarization? (2) What is the contribution of polarization-induced electrostatic interactions to the binding free energy in avidin–biotin? In this work, the MM/PBSA method⁴⁰ is used to obtain the free energies of avidin binding to biotin (BTN1) and 2'-iminobiotin (BTN2) (structures shown in Figure 1) under respectively AMBER charges and PPC, in order to explicitly investigate the effect of protein polarization.

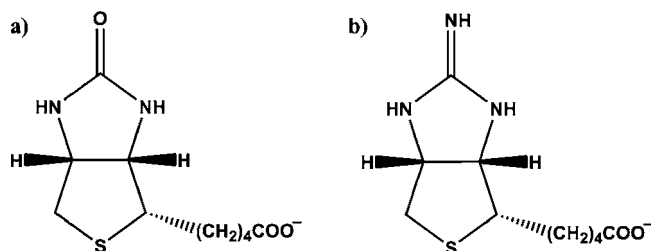


Figure 1. Structures of the two biotin analogues studied: (a) biotin (BTN1) and (b) 2'-iminobiotin (BTN2).

Theoretical Approach

Polarized Protein-Specific Charge. The PPC is obtained by restricted fitting to electrostatic potential (RESP)^{41–43} in continuum solvent, using the self-consistent molecular fragmentation with conjugate caps Poisson–Boltzmann (MFCC-PB) method. A detailed description of this method can be found in ref 27. Here, we only give a brief summary for clarity. In our approach, the protein is decomposed into residue-based fragments to which proper caps are added to saturate the covalent bonds and mimic the chemical environment. The electron density of each fragment is obtained through quantum mechanical calculation at the B3LYP/6-31G* level. In the QM calculation of each fragment, other residues are taken as background charges to include the intra-protein polarization effect. The partial charges on each atom of protein generated from the MFCC/RESP are passed to the PB solver Delphi program⁴⁴ to generate discrete induced charges on the cavity surface. The dielectric solute/solvent boundary is defined by AMBER as the van der Waals (vdW) radii⁴⁵ of solute atoms with a probe radius of 1.4 Å. The internal dielectric constant is set to unity and that of the solvent to 80. The grid density is set to 4.0 grids/Å in the PB calculation. Surface charges mimicking the solvation effect are then taken as additional background charges into the next cycle of QM calculations to fit new atomic charges. The solute and solvent polarize each other until convergence is reached, when the dipole of the protein and the surface charges are both the same within a pre-assigned numerical accuracy. This procedure basically follows the self-consistent reaction field (SCRf) theory, except that the generation of ESP on the solute–solvent surface is based on the MFCC scheme. Also, multibody effect are included in the final PPC. All QM calculations are performed with Gaussian03 software.⁴⁶

Initial Structures. The initial structure of avidin–BTN1 is taken from the Protein Data Bank (PDB ID: 1AVD). Hydrogen atoms are added using the Leap module in Amber 9. Since the crystal structure of the BTN2/avidin complex is not available, we adopt the same method as Kuhn et al.^{37,38} used to generate its structure. The guanidinium group in BTN2 is set to the neutral form.^{11,47,48} Thus, both BTN1 and BTN2 have negative charge of $-1e$. The protein–ligand complex is soaked in a periodic box of TIP3P water, and the minimum distance from the atom to the surface of the box is set to 10 Å. Counterions are added to neutralize the whole system. The structures of the ligands (BTN1 and BTN2) are optimized at

- (20) He, X.; Zhang, J. Z. H. *J. Chem. Phys.* **2006**, *124*, 184703.
 (21) Deev, V.; Collins, M. A. *J. Chem. Phys.* **2005**, *122*, 154102.
 (22) Li, S. H.; Li, W.; Fang, T. *J. Am. Chem. Soc.* **2005**, *127*, 7215–7226.
 (23) Bettens, R. P. A.; Lee, A. M. *J. Phys. Chem. A* **2006**, *110*, 8777–8785.
 (24) Wang, B.; Merz, K. M. *J. Chem. Theory Comput.* **2006**, *2*, 209–215.
 (25) Xie, W. S.; Gao, J. L. *J. Chem. Theory Comput.* **2007**, *3*, 1890–1900.
 (26) Xie, W. S.; Song, L. C.; Truhlar, D. G.; Gao, J. L. *J. Phys. Chem. B* **2008**, *112*, 14124–14131.
 (27) Ji, C. G.; Mei, Y.; Zhang, J. Z. H. *Biophys. J.* **2008**, *95*, 1080–1088.
 (28) Zhang, D. W.; Zhang, J. Z. H. *J. Chem. Phys.* **2003**, *119*, 3599–3605.
 (29) Gao, A. M.; Zhang, D. W.; Zhang, J. Z. H.; Zhang, Y. K. *Chem. Phys. Lett.* **2004**, *394*, 293–297.
 (30) Mei, Y.; Zhang, D. W.; Zhang, J. Z. H. *J. Phys. Chem. A* **2005**, *109*, 2–5.
 (31) Mei, Y.; Ji, C. G.; Zhang, J. Z. H. *J. Chem. Phys.* **2006**, *125*, 94906.
 (32) Ji, C. G.; Zhang, J. Z. H. *J. Am. Chem. Soc.* **2008**, *130*, 17129–17133.
 (33) Duan, L. L.; Mei, Y.; Zhang, Q. G.; Zhang, J. Z. H. *J. Chem. Phys.* **2009**, *130*, 115102.
 (34) Ji, C.; Zhang, J. *J. Phys. Chem. B* **2009**, *113*, 13898–13900.
 (35) Tong, Y.; Ji, C. G.; Mei, Y.; Zhang, J. Z. H. *J. Am. Chem. Soc.* **2009**, *131*, 8636–8641.
 (36) Green, N. M. *Biochem. J.* **1963**, *89*, 585–591.
 (37) Kuhn, B.; Kollman, P. A. *J. Med. Chem.* **2000**, *43*, 3786–3791.
 (38) Kuhn, B.; Kollman, P. A. *J. Am. Chem. Soc.* **2000**, *122*, 3909–3916.
 (39) DeChancie, J.; Houk, K. N. *J. Am. Chem. Soc.* **2007**, *129*, 5419–5429.
 (40) Kollman, P. A. *Chem. Rev.* **1993**, *93*, 2395–2417.

- (41) Bayly, C. I.; Cieplak, P.; Cornell, W. D.; Kollman, P. A. *J. Phys. Chem.* **1993**, *97*, 10269–10280.
 (42) Cieplak, P.; Cornell, W. D.; Bayly, C.; Kollman, P. A. *J. Comput. Chem.* **1995**, *16*, 1357–1377.
 (43) Cornell, W. D.; Cieplak, P.; Bayly, C. I.; Kollman, P. A. *J. Am. Chem. Soc.* **1993**, *115*, 9620–9631.
 (44) Rocchia, W.; Sridharan, S.; Nicholls, A.; Alexov, E.; Chiabrera, A.; Honig, B. *J. Comput. Chem.* **2002**, *23*, 128–137.
 (45) Cornell, W. D.; Cieplak, P.; Bayly, C. I.; Gould, I. R.; Merz, K. M.; Ferguson, D. M.; Spellmeyer, D. C.; Fox, T.; Caldwell, J. W.; Kollman, P. A. *J. Am. Chem. Soc.* **1995**, *117*, 5179–5197.
 (46) Frisch, M. J.; et al. *Gaussian 03, Revision D.01*; Gaussian Inc.: Wallingford, CT, 2004.
 (47) Green, N. M. *Biochem. J.* **1966**, *101*, 774–780.
 (48) Green, N. M. *Adv. Protein Chem.* **1975**, *29*, 85–133.

the HF/6-31G** level, and their atomic charges are fitted through RESP at the B3LYP/cc-PVTZ level. AMBER03^{49,50} and the generalized Amber force field (GAFF)⁵¹ are employed for protein and ligand, respectively. The particle mesh Ewald (PME) method⁵² is used to treat long-range electrostatic interactions, while a typical 12 Å cutoff is used for the vdW interactions. Hydrogen atoms in BTN1/avidin and all atoms in BTN2/avidin are optimized, as well as water molecules. Because the structure of BTN2/avidin is built from BTN1/avidin, optimization of heavy atoms is necessary. Superposition of these two optimized structures indicates that there are no large deviations between these two structures, except for the residues between VAL103 and THR113, which are far from the ligand binding pocket and insert into the bulk water. Polarized protein-specific charges of avidin/BTN1 and avidin/BTN2 complexes are calculated on the basis of these two optimized structures.

Molecular Dynamics. The initial structures for the MD simulation are obtained as described above. The systems are relaxed in a two-step equilibration procedure. In the first step, only the solvent molecules are optimized using the steepest descent minimization, followed by conjugate gradient minimization. In the second step, the complex system is optimized until convergence is reached. After this two-step equilibration, the systems are heated from 0 to 300 K in 100 ps, followed by 1 ns NPT simulation with a time step of 2 fs. Nonbond interactions are treated as described in the above. Langevin⁵³ dynamics is applied to control the temperature, with a collision frequency of 1.0 ps⁻¹. The SHAKE algorithm is employed to restrain all bonds involving hydrogen atoms. The AMBER03 force field is employed for protein and GAFF is used for ligands. In simulations using PPC, the atomic charges are replaced by PPC while keeping other parameters and simulation conditions intact.

MM/PBSA. In the MM/PBSA calculation, the average total free energy of the system, G , is evaluated as

$$G = G_{\text{PBSA}} - TS_{\text{solute}} \\ = E_{\text{es}} + G_{\text{PB}} + E_{\text{vdW}} + G_{\text{np}} - TS_{\text{solute}}$$

where G is decomposed into contributions from electrostatic (E_{es}), van der Waals (E_{vdW}), polar solvation (G_{PB}), nonpolar solvation (G_{np}), and entropy (TS_{solute}) term. The binding free energy of a noncovalent association, ΔG_{bind} , can be computed as

$$\Delta G_{\text{bind}} = G_{\text{complex}} - G_{\text{receptor}} - G_{\text{ligand}}$$

or

$$\Delta G_{\text{bind}} = \Delta G_{\text{PBSA}} - T\Delta S_{\text{solute}} \\ = \Delta E_{\text{es}} + \Delta G_{\text{PB}} + \Delta E_{\text{vdW}} + \Delta G_{\text{np}} - T\Delta S_{\text{solute}}$$

The difference in binding free energy, $\Delta\Delta G$, between BTN1 and BTN2 is given by

$$\Delta\Delta G = \Delta G_{\text{BTN2}} - \Delta G_{\text{BTN1}}$$

In this work, MD simulation is performed for avidin–biotin complexes using respectively PPC and AMBER03 charge. One hundred snapshots from the last 200 ps of the simulation at 2 ps intervals are extracted for MM/PBSA calculation. The PB calculation is performed with the Delphi program using PARSE atomic radii.⁵⁴ The interior and exterior dielectric constants are set to 1

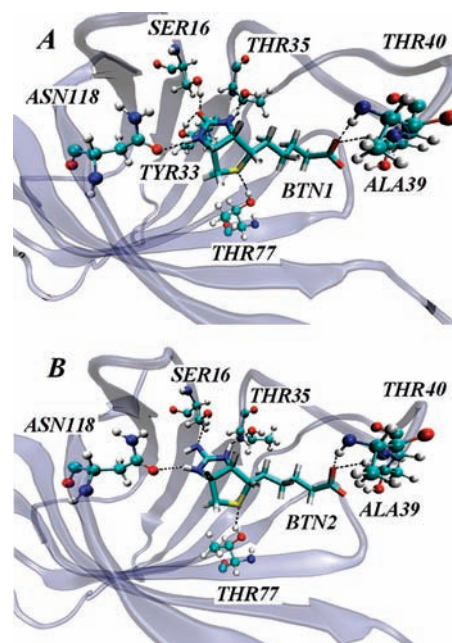


Figure 2. Hydrogen-bonding network at the binding site of avidin–BTN1 (A) and avidin–BTN2 (B). BTN1 and BTN2 are shown in stick representation, avidin in cartoon, and the residues forming H-bonds with BTN1 and BTN2 in ball-and-stick.

and 80, respectively. A grid spacing of 0.5 Å is used. G_{np} is calculated from $G_{\text{np}} = \gamma_{\text{SA}} + b$ [where $\gamma = 0.00542 \text{ kcal}/(\text{mol} \cdot \text{Å}^2)$ and $b = 0.92 \text{ kcal/mol}$] using *molsurf*⁵⁵ to calculate the surface area. Entropy loss during protein–ligand binding is calculated using the *nmode*⁵⁶ module in AMBER9.

Results and Discussion

The bicyclo rings of BTN1 and BTN2 are both deeply buried inside the protein, thereby forming several hydrogen bonds and favorable vdW interactions with avidin. Avidin has a nearly ideal cavity for biotin binding, surrounding it with four tryptophan residues. As shown in Figure 1, the structures of BTN1 and BTN2 are very similar to each other, differing only in the headgroup, with BTN2 being a less favorable hydrogen bond acceptor than BTN1. BTN1 and BTN2 form respectively seven and six hydrogen bonds with avidin (Figure 2). They have very similar binding modes. The disappearance of a hydrogen bond on going from BTN1 to BTN2 may be responsible for the large difference in binding free energy of about 6 kcal/mol.⁴⁸ Thus, rigorous study of the interaction in these complexes is required to find the origin of this loss of binding affinity. Since the electrostatic environment of the binding site changes as the ligand is varied, it is important to capture such electrostatic changes in the free energy calculation.

Polarized protein-specific charges provide more reliable electrostatic interactions in the complexes. Comparison of PPC with AMBER03 charges in Figure 3a,b shows obvious differences. Due to polarization from ligand binding, a protein possesses slightly different charges when binding to different ligands. This polarization effect can be more pronounced for charged ligands such as biotin. In Figure 3c, the difference in PPC of avidin on binding with BTN1 and BTN2 is shown for

(49) Duan, Y.; Wu, C.; Chowdhury, S.; Lee, M. C.; Xiong, G. M.; Zhang, W.; Yang, R.; Cieplak, P.; Luo, R.; Lee, T.; Caldwell, J.; Wang, J. M.; Kollman, P. A. *J. Comput. Chem.* **2003**, *24*, 1999–2012.

(50) Lee, M. C.; Duan, Y. *Proteins* **2004**, *55*, 620–634.

(51) Wang, J.; Wolf, R. M.; Caldwell, J. W.; Kollman, P.; Case, D. A. *J. Comput. Chem.* **2004**, *25*, 1157–1174.

(52) Darden, T.; York, D.; Pedersen, L. *J. Chem. Phys.* **1993**, *98*, 10089–10092.

(53) Pastor, R. W.; Brooks, B. R.; Szabo, A. *Mol. Phys.* **1988**, *65*, 1409–1419.

(54) Sitkoff, D.; Sharp, K.; Honig, B. *J. Phys. Chem.* **1994**, *98*, 1978–1988.

(55) Connolly, M. L. *J. Appl. Crystallogr.* **1983**, *16*, 548–558.

(56) Nguyen, D. T.; Case, D. A. *J. Phys. Chem.* **1985**, *89*, 4020–4026.

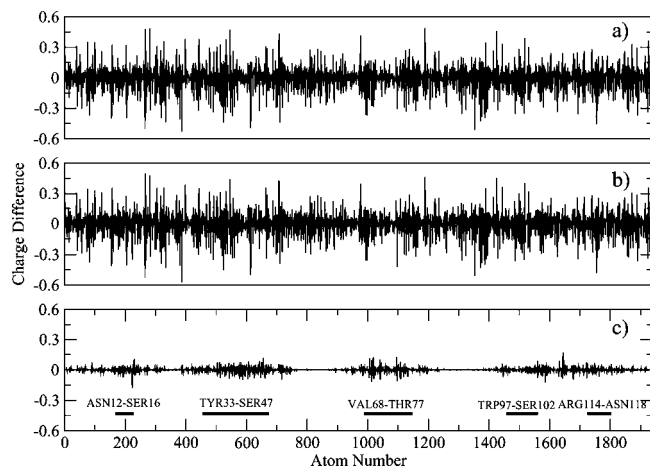


Figure 3. (a) Charge difference between PPC and AMBER03 for avidin in complex with BTN1. (b) The same as (a) except for complex with BTN2. (c) Difference in PPC for avidin in complex with BTN1 and BTN2. Residues around the binding pocket are labeled explicitly.

direct comparison. It can be seen that the difference in PPC of avidin for two complexes is generally very small, but there is a noticeable difference for residues around the binding pocket and those extending into water, with large deviations in the two complexes. These observations convince us that using PPC in the MD simulation can better differentiate the electrostatic environment and thus improve both the energetics and dynamics for protein–ligand binding, such as that in an avidin–biotin complex.

Our detailed analysis of interaction energy indicates that residues showing large differences in interactions are all around the binding pocket, and PPC generally gives more attractive electrostatic interaction between protein and ligands than AMBER03 charge does. In particular, the interaction of ALA39 with BTN1 or BTN2 is the strongest among all residues, and it shows the largest difference under PPC and AMBER03 charge. It is shown that the carboxylate anion of BTN1 and BTN2 plays an important role in binding with ALA39. As the carboxylate anion is negatively charged, the electrostatic interactions of ALA39 with BTN1 and BTN2 are quite strong, and the hydrogen bonds formed between them are very stable.

The specific structural change in local binding region during MD simulation is important to protein–ligand binding energy, in particular for crucial hydrogen bonds. Figure 4 shows the time evolution of several hydrogen bond lengths during MD simulation. It is noticed that hydrogen bonds under PPC are generally more stable (with less fluctuation) than those under AMBER03 charge during MD fluctuation. This is due to the polarization effect embedded in PPC, which has been analyzed in the study of other proteins recently.³³ Among these hydrogen bonds, we notice in particular that the one formed between the carbonyl group in BTN1 and the hydroxyl group in TYR33 is loose in the MD simulation under AMBER charge, while it remains very stable under PPC over long simulation times. Since this hydrogen bond does not exist in avidin–BTN2 binding, it is shown to be mainly responsible for the increased binding affinity of avidin–biotin over that of avidin–BTN2 (about 6 kcal/mol). Specific energy decomposition proves this argument, as the data in tabulated in the Supporting Information shows that it contributes over 10 kcal/mol in electrostatic interaction in the MD simulation under PPC, but no contribution under AMBER charges. The important effect of electrostatic polariza-

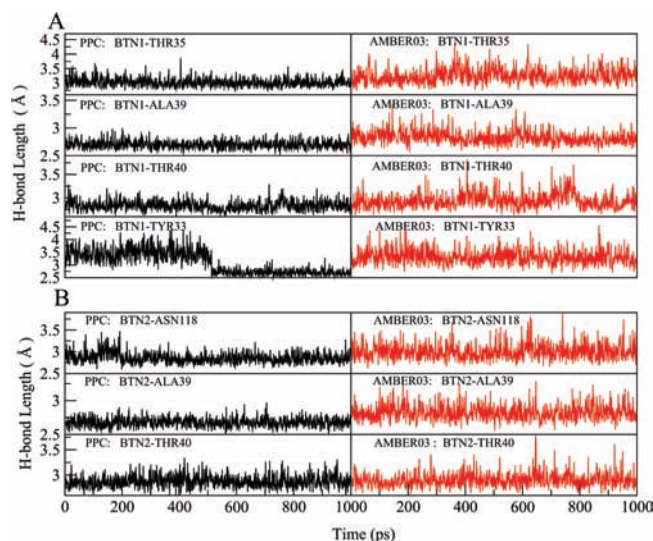


Figure 4. Time evolution of hydrogen bond lengths between avidin and the ligands during MD simulation. (A) Four hydrogen bonds between BTN1 and avidin, including BTN1–THR35, BTN1–ALA39, BTN1–THR40, and BTN1–TYR33. (B) Three hydrogen bonds formed by BTN2 and avidin, including BTN2–ASN118, BTN2–ALA39, and BTN2–THR40. The results from PPC and AMBER03 are shown in black and red, respectively.

tion on the stability of hydrogen bonds has also been observed in previous studies.^{33,34}

Additionally, as is shown in Figure 5, the local structure of avidin/BTN1 at residues ASN118–ILE119 changes from a β strand (Thr113–Arg122) to a coil during MD simulation under AMBER03 force field. However, this unreal denaturation of the β strand does not occur in simulation using PPC. This is again evidence that the lack of electronic polarization artificially weakens the hydrogen bonds in the standard force field and causes partial denaturation of the local secondary structure in protein.^{32,33} Thus, using PPC in MD simulation should better preserve the local structures and give more reliable structural ensembles for dynamical analysis than using AMBER charges near the native structures. Additionally, this partial denaturation does not occur in the avidin–BTN2 system under either AMBER or PPC simulation.

The trajectories extracted from MD simulation are used for MM/PBSA calculation of binding free energy. Since MM/PBSA calculation gives direct information on absolute binding energies, we use both PPC and AMBER charges in MM/PBSA calculation and compare the result between them. Table 1 summarizes the calculated free energies and their various components for binding of BTN1 and BTN2 to avidin under both PPC and AMBER charges, respectively. Analysis of the results provides some important information on the mechanism of avidin binding to biotin and its analogue. First, it shows that the calculated difference in free energies of binding avidin to BTN1 and BTN2 is 8.4 kcal/mol under PPC, which is reasonably close to the experimentally measured value of 6.1 kcal/mol. For comparison, the calculated free energy difference under AMBER03 charge is only 0.32 kcal/mol, which essentially fails to differentiate the large free energy difference in binding of avidin to these two similar ligands. In particular, both the vdW and electrostatic contributions to avidin binding to BTN1 and BTN2 are essentially the same under the AMBER03 force field. For comparison, we also list the free energy computed by Kuhn,^{37,38} which gives a difference in binding free energy of 2.7 kcal/mol under AMBER94 force field. To put things in perspective, we

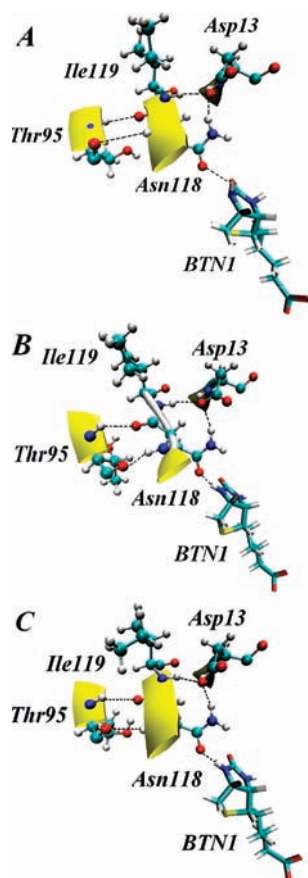


Figure 5. A piece of β strand containing Asn118 and Ile119 in BTN1: (A) native structure, (B) final denatured structure (β sheet changes into coil structure) in MD simulation under AMBER03 charge, and (C) final structure of the binding complex from MD simulation under PPC.

should keep in mind that the newer AMBER03 has been shown to provide more reliable structure ensembles.⁵⁷ Furthermore, in Kuhn's calculations, only one subunit of avidin is allowed to move in the MD simulation, while the other three are fixed. In the present simulation, all four subunits are free to move. These two factors may be responsible for the observed difference in calculated binding free energy under two AMBER force fields.

One should keep in mind, however, that since entropy calculations from the normal-mode approach in MM/PBSA are sometimes less reliable, there are uncertainties in the calculated free energies. However, our simulation shows a negligible difference in entropy loss upon avidin binding to BTN1 and

BTN2, ranging from 1.2 kcal/mol in the PPC simulation to 1.8 kcal/mol in the AMBER03 simulation. This can be understood by the fact that BTN1 and BTN2 are very similar in structure and thus there is no entropy difference in binding of avidin to either of them. To further strengthen our argument, we applied a more rigorous thermodynamic integration (TI) method to calculate the relative binding free energy between BTN1 and BTN2 to avidin under AMBER03 force field. In the TI calculation, only atoms in the ureido group are mutated from those in BTN1 to those in BTN2, which follows the same procedure as in ref 38. Gaussian quadrature with nine nodes (λ) and soft-core potential⁵⁸ are employed to smoothly switch the ligand. At each λ , the whole system is first minimized for 500 steps and then heated to 300 K in 250 ps, followed by 100 ps equilibration. For switching BTN1 to BTN2 in protein, a 1 ns production run is performed for final analysis. For the system in water, a 200 ps production run is sufficient to give a converged result. Our result shows that the difference in binding free energy between BTN1 and BTN2 is only 0.9 kcal/mol, which is quite consistent with our MM/PBSA calculation. More detailed results of the TI calculation will be reported in a subsequent paper.

By eliminating the entropy factor, we can now focus on the electrostatic contribution to binding free energy in the avidin–biotin complex. We thus examine in Table 1 the relevant electrostatic contribution to binding free energies. We see that under both AMBER03 and AMBER94, electrostatic interaction ΔE_{es} (although substantial) and electrostatic solvation energy ΔG_{PB} nearly cancel each other in avidin binding to both BTN1 and BTN2. The overall electrostatic contribution to free energy is actually somewhat unfavorable (positive) by about 4 kcal/mol, as shown in the fifth column in Table 1. This had led to the conclusion by authors in refs 37 and 38 that association between avidin and biotin is mainly driven by van der Waals interactions. In contrast, however, calculation under PPC shows that the electrostatic interaction makes a substantial contribution to the free energy of avidin–biotin binding. In particular, the combined electrostatic contribution to the free energy is almost -10 kcal/mol in the avidin–biotin system, but much less (-1.7 kcal/mol) in the avidin–BTN2 system. This result gives strong evidence that electrostatic interaction actually makes a substantial contribution to the free energy of avidin–biotin binding, which is in direct contrast to the previous understanding given by authors in refs 37 and 38. Interestingly, the electrostatic interaction does not make important contribution to free energy of avidin binding to the analogous BTN2. Thus electrostatic interaction almost entirely accounts for the observed difference in free energy between avidin binding to BTN1 and that to

Table 1. Components of the Binding Free Energy between Avidin and the Two Ligands BTN1 and BTN2 Using PPC and Amber03 Charge^a

	ligand	ΔE_{es}	ΔG_{PB}	$\Delta(E_{\text{es}} + G_{\text{PB}})$	ΔE_{vdW}	ΔG_{np}	ΔG_{PBSA}	$\Delta\Delta G_{\text{PBSA}}^e$	$-T\Delta S$	$\Delta(-T\Delta S)^f$	ΔG	$\Delta\Delta G$
PPC	BTN1	-227.0	217.1	-9.9	-27.6	-3.2	-40.7	7.1	17.3	1.2	-23.4	8.4
	BTN2	-216.3	214.6	-1.7	-28.6	-3.3	-33.6		18.5		-15.1	
A03 ^b	BTN1	-183.8	188.1	4.4	-31.4	-3.3	-30.3	-1.4	18.9	1.8	-11.4	0.3
	BTN2	-183.7	184.8	1.2	-29.6	-3.3	-31.7		20.7		-11.1	
A94 ^c	BTN1	-154.4	158.5	4.1	-36.4	-3.5	-35.8	1.0	18.1	1.7	-17.7	2.7
	BTN2	-163.4	168.5	5.1	-36.4	-3.5	-34.8		19.8		-15.0	
exp ^d	BTN1										-20.4	6.1
	BTN2										-14.3	

^a All energies are in kcal/mol. $\Delta\Delta G_{\text{bind}}$ is the difference of ΔG between BTN1 and BTN2. ^b AMBER03 force field. ^c AMBER94 force field by Kuhn et al.³⁷ ^d See ref 36. ^e $\Delta\Delta G_{\text{PBSA}} = \Delta G_{\text{PBSA}}^{\text{BTN2}} - \Delta G_{\text{PBSA}}^{\text{BTN1}}$. ^f $\Delta(-T\Delta S) = -T\Delta S_{\text{BTN2}} - (-T\Delta S_{\text{BTN1}})$.

BNT2. Comparing the result from PPC calculation and that from AMBER charge, it is clear that the difference in calculated electrostatic contributions is due to the polarization effect, which is missing in the AMBER force field. As is discussed above, the hydrogen bond between BTN1 and TYR33 is the major contributing factor to the enhanced binding affinity in avidin–biotin under PPC simulation. Since this hydrogen bond is much less stable under AMBER charge, simulation under AMBER03 failed to distinguish the binding affinity of avidin to BTN1 and BTN2.

Conclusions

The present work provided fresh evidence that protein polarization is critical to accurately describing protein–ligand binding structure and giving correct relative free energies in binding of avidin to biotin and its analogue BTN2. In particular, we find that the polarization-induced electrostatic interaction makes a substantial contribution to the free energy of avidin–biotin binding, in contrast to the common belief that electrostatics does not contribute to the binding free energy of this benchmark system. The stabilization of the hydrogen bond between BTN1 and TYR33, which does not exist in the avidin–BTN2 complex, and the electrostatic interaction between biotin and nearby residues are responsible for the enhanced binding affinity in avidin–biotin over that in avidin–BTN2. The earlier conclusion about the lack of electrostatic interaction in avidin–biotin binding^{37,38} is the result of using a nonpolarizable force field, which fails to take into account the polarization effect in the protein–ligand complex. In the analogous

avidin–BTN2 system, however, electrostatics does not make an observable contribution to the free energy of binding. This helps to explain the observed large difference in binding free energy (6.1 kcal/mol) between the two systems. It is the polarization energy that makes a significant difference in their binding free energies. We also discovered that, without polarization effect included in the simulation, some specific local structure in the avidin–biotin complex is partially denatured due to the weakening of intra-protein hydrogen bonds.

A note is in order here for possible further improvement of PPC. Since proteins are dynamic and exist as ensembles of structures, it may be desirable to fit PPC on-the-fly or to use multiple configurations. One may also imagine employing explicit water model instead of the implicit PB method, thus including the solvent fluctuation effect in multiconfiguration fitting of PPC.^{59,60} These ideas need to be explored in future studies.

Acknowledgment. This work is partially supported by the National Science Foundation of China (Grants No. 20773060, 20803034, and 20933002) and Shanghai PuJiang program (09PJ1404000).

Supporting Information Available: Tables showing the interaction between ligands and nearby residues; complete ref 46. This material is available free of charge via the Internet at <http://pubs.acs.org>.

JA909575J

(57) Lwin, T. Z.; Luo, R. *Protein Sci.* **2006**, *15*, 2642–2655.

(58) Steinbrecher, T.; Mobley, D. L.; Case, D. A. *J. Chem. Phys.* **2007**, *127*, 214108.

(59) Gao, J. L.; Luque, F. J.; Orozco, M. *J. Chem. Phys.* **1993**, *98*, 2975–2982.

(60) Sanchez, M. L.; Aguilar, M. A.; delValle, F. J. O. *J. Comput. Chem.* **1997**, *18*, 313–322.